*Title Page

A New Radial Symmetry Measure Applied to Photogrammetry

Authors
Raquel Dosil, Xosé M. Pardo, Xosé R. Fdez-Vidal,
Antón García-Díaz, Víctor Leborán

Centro de Investigación en Tecnoloxías da Información (CITIUS), Universidade de Santiago de Compostela, Campus Universitario Sur, s/n, 15782, Santiago de Compostela, Spain

email: raquel.dosil@usc.es
Phone: +34 881813578
Fax: +34 881814112

Abstract

This work presents a new measure for radial symmetry and an algorithm for its computation. This measure identifies radially symmetric blobs as locations with contributions from all orientations at some scale. Hence, at a given scale, radial symmetry is computed as the product of the responses of a set of even symmetric feature detectors, with different orientations. This operator presents low sensitivity to shapes lacking radial symmetry, is robust to noise, contrast changes and strong perspective distortions, and shows a narrow point spread function. A multiresolution measure is provided, computed as the maximum of the symmetry measure evaluated over a set of scales.

We have applied this measure in the field of photogrammetry, for the detection of circular coded fiducial targets. The detection of local maxima of multirresolution radial symmetry is combined with a step of false positive rejection, based on elliptical model fitting. In our experiments, the efficiency of target detection with this method is improved regarding a well-known commercial system, which is expected to improve the performance of bundle adjustment techniques. In order to fulfill all steps previous to bundle adjustment, we have also developed our own method for recognition of coded targets. This is accomplished by a standard procedure of segmentation and decoding of the ring sequence. Nevertheless, we have included a step for the verification of false positives of decoding based on correlation with reference targets. As far as we know, this approach cannot be found in literature.

Keywords: *circular coded targets; radial symmetry; filter banks; log Gabor; target identification; correlation.*

Originality and Contribution

We have developed a new measure for radial symmetry and an algorithm for its computation. Our measure identifies radially symmetric blobs as locations with contributions from all orientations at some scale. Hence, at a given scale, radial symmetry is computed as the product of the responses of a set of even symmetric feature detectors, with different orientations. In this way, the response of this detector will vanish at locations with contributions from a subset of oriented features, thus avoiding weak responses from non radially symmetric shapes. This operator presents low sensitivity to shapes lacking radial symmetry, is robust to noise, contrast changes and strong perspective distortions, and shows a narrow point spread function. A multiresolution measure is provided, computed as the maximum of the symmetry measure evaluated over a set of scales.

We have applied this measure in the field of photogrammetry, for the detection of circular coded fiducial targets. Research in photogrammetry is usually focused on the development of robust bundle adjustment methods, while previous steps for location and identification of targets receive little attention. Here, we propose to facilitate bundle adjustment by reducing the number of detection errors through the use of our radial symmetry detector. Candidate target locations are computed as the local maxima of the proposed multiresolution radial symmetry measure, followed by false positive rejection by means of standard elliptical model fitting and thresholding of the fitting error. In our experiments, the efficiency of target detection with this method is improved regarding a well-known commercial system.

In order to fulfill all steps previous to bundle adjustment, we have also developed our own method for identification of coded targets. This is accomplished by a standard procedure of segmentation and decoding of the ring sequence. Nevertheless, we have included a step for the verification of false positives of decoding based on correlation with reference targets. As far as we know, this approach cannot be found in literature.

A New Radial Symmetry Measure Applied to Photogrammetry

Abstract

This work presents a new measure for radial symmetry and an algorithm for its computation. This measure identifies radially symmetric blobs as locations with contributions from all orientations at some scale. Hence, at a given scale, radial symmetry is computed as the product of the responses of a set of even symmetric feature detectors, with different orientations. This operator presents low sensitivity to shapes lacking radial symmetry, is robust to noise, contrast changes and strong perspective distortions, and shows a narrow point spread function. A multiresolution measure is provided, computed as the maximum of the symmetry measure evaluated over a set of scales.

We have applied this measure in the field of photogrammetry, for the detection of circular coded fiducial targets. The detection of local maxima of multirresolution radial symmetry is combined with a step of false positive rejection, based on elliptical model fitting. In our experiments, the efficiency of target detection with this method is improved regarding a well-known commercial system, which is expected to improve the performance of bundle adjustment techniques. In order to fulfill all steps previous to bundle adjustment, we have also developed our own method for recognition of coded targets. This is accomplished by a standard procedure of segmentation and decoding of the ring sequence. Nevertheless, we have included a step for the verification of false positives of decoding based on correlation with reference targets. As far as we know, this approach cannot be found in literature.

Keywords: *circular coded targets; radial symmetry; filter banks; log Gabor; target identification; correlation.*

1. Introduction

Many applications of computer vision require the detection of circular shapes. Examples of this are photogrammetry and robot navigation, which are usually based on the detection of fiducial targets. In general, under perspective distortion, an elliptical model is assumed to provide a good approach to the observed shape of a circular target. A common ellipse detection technique is the convolution with circular template filters. In [6], the use of the Laplacian of Gaussian (LoG) filter is proposed as a blob detector due to its radial symmetry. Multiresolution blob detection is achieved by generating a scale space of LoG and maximizing their response over scales. A different approach is that of voting based algorithms, where contour points vote an accumulator in the location of possible central positions of the shape. Examples of this are the fast radial symmetry

detector by Loy and Zelinsky [7], or the rotation and scaling invariant Hough ellipse detector by Nixon and Aguado [8].

The above mentioned algorithms present different problems. Blob detectors do not usually offer a precise shape definition, being sensitive to very different kinds of shapes. Voting based algorithms are not invariant to scale, since the intensity of their response depends on the number of pixels on the contour of the shape. Furthermore, they produce artifacts, given that each contour point votes many possible centre locations [8]. The fast radial symmetry detector [7] solves this problem by having into account the intensity of the contours, and also by imposing strong constraints on the circularity of the shape, at the expense of a lack of robustness to perspective distortion –ellipticity. On the other hand, the main drawbacks of the different approaches to the Hough transform of ellipses are related to high computational cost and wide point spread functions.

To cope with these problems, we propose a novel technique to measure radial symmetry that presents low sensitivity to shapes lacking radial symmetry, is robust to noise, contrast changes and strong perspective distortions, and shows a narrow point spread function. The main idea behind this detector is to consider radially symmetric blobs as region features with contributions from all orientations at a given scale. We also provide an algorithm for the computation of this measure. To detect blobs with these characteristics, we design a radially symmetric blob detector as the product of a set of features with even phase, same size, but different orientations. Like in [6], to get scale invariance, we compute a scale space of radially symmetric blobs and, subsequently, we obtain the overall symmetry response by maximization over scales.

In a way, this is similar to the LoG blob detector in [6]. The LoG can be thought of as being integrating the information from all orientations at a given scale to produce a radially symmetric template. Such integration can be approximated as the addition of all orientations, instead of the product. The result is an operator with a strong response to radially symmetric patterns, but also with weak responses to any other kind of oriented patterns. On the other hand, the product of orientations provides strong responses only to patterns that contain each and every orientation, as shown in Figure 2. That is, weak responses to non-symmetric patterns are eliminated.

a) b)

Figure 1. Examples of Photomodeler Scanner® and AICON 3D® landmarks. a) Non-coded landmarks b) 8-bit coded landmarks, with opposite contrast.

We have applied this radial symmetry measure in the field of photogrammetry. Most commercial photogrammetry systems are based on the use of circular targets that usually show high contrast patterns. Coded reference targets present unique designs that allow reliable matching among different views for image registration. Non-coded targets are identical and are used to precisely locate points on the object's surface. Popular commercial photogrammetry systems, like Photomodeler Scanner® and AICON 3D®, use circular targets like the ones shown in Figure 1. Non-coded targets are simply black circles over white background, or vice versa. Coded targets present an outer ring that is divided into segments (bits). Each segment can be either black or white (0/1 or vice versa), forming a binary sequence that is unique for each coded landmark.

Although the accuracy of target detection, location and recognition is very important for bundle adjustment methods, most state-of-the-art applications use quite simple approaches. Target candidate selection is often simply accomplished through segmentation of the image by thresholding [1][2][3][4]. This is possible since controlled scenarios and illumination conditions are assumed or forced. Heuristic post-processing might then be applied for outlier rejection, based on geometric parameters of the detected blobs, like size, perimeter, aspect ratio, error of fitting, etc. Regarding the recognition of coded targets –decoding–, high contrast and known geometry of the coded rings make it possible to use straightforward decoding techniques, based on the segmentation of the outer ring [5][1][2].

Here, we propose to apply our radial symmetry measure to provide a robust circular target detector that reduces the number of detection errors, hence facilitating bundle adjustment. ~~We will show that, as a circular target detector, our radial symmetry measure is robust to noise, contrast, scale and perspective distortion, and it presents low sensitivity to non-circular coded targets.~~ To do so, we have developed a system that fulfills all steps previous to bungle adjustment: detection, location and recognition of

circular targets. The general diagram of the system is shown in Figure 3. Detection is accomplished by computing local maxima of the response of the proposed symmetry measure. The precision location of the center of the landmark is performed using state-of-the-art techniques, which involve extracting a region of interest around each local maximum of the symmetry measure, with size depending on the scale of the feature, followed by elliptical model fitting of the contours found in the region of interest. Finally, to carry out coded target recognition we have developed a procedure that, up to our knowledge, can not be found in literature before. It starts with a standard procedure of segmentation and decoding of the outer coded ring, but incorporates a further step of false classification rejection, through the computation of the correlation of the ring area with a synthetic reference image of the coded ring. The whole system has been validated in realistic scenarios and its results have been compared to a popular commercial photogrammetry system, AICON 3D, showing improved detection and recognition rates.

The rest of the paper is organized as follows. The implementation details of our radially symmetric blob detector and the proposed target detection system are described in section 2, while the technique employed for coded target identification is presented in section 3. Section 4 presents the experimental setup for validation, the experimental results and their discussion. Conclusions are summarized in section 5.

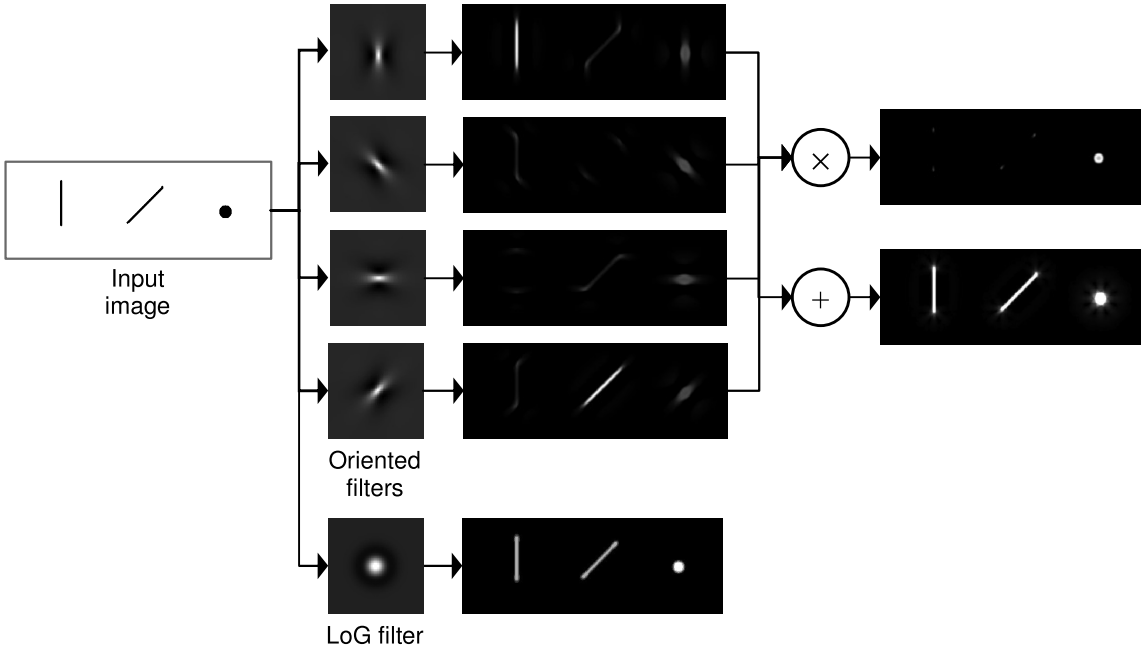

Figure 2. Columns from left to right: 1) Input image, showing two linear shapes, with different orientations, and a circular shape. 2) Visualization of the masks of several orientation selective filters, and also a LoG filter. 3) Responses of each of the filters to the input image. Oriented filters show strong responses only to shapes with similar orientation and also to the circular shape –which contains all orientations. The LoG filter presents responses to all of the shapes. 4) Product and addition of oriented filter responses. The result of the addition is similar to the response of the LoG filter. The product vanishes in case of shapes with just one orientation, while it is strong and well localized in the case of the circular shape.

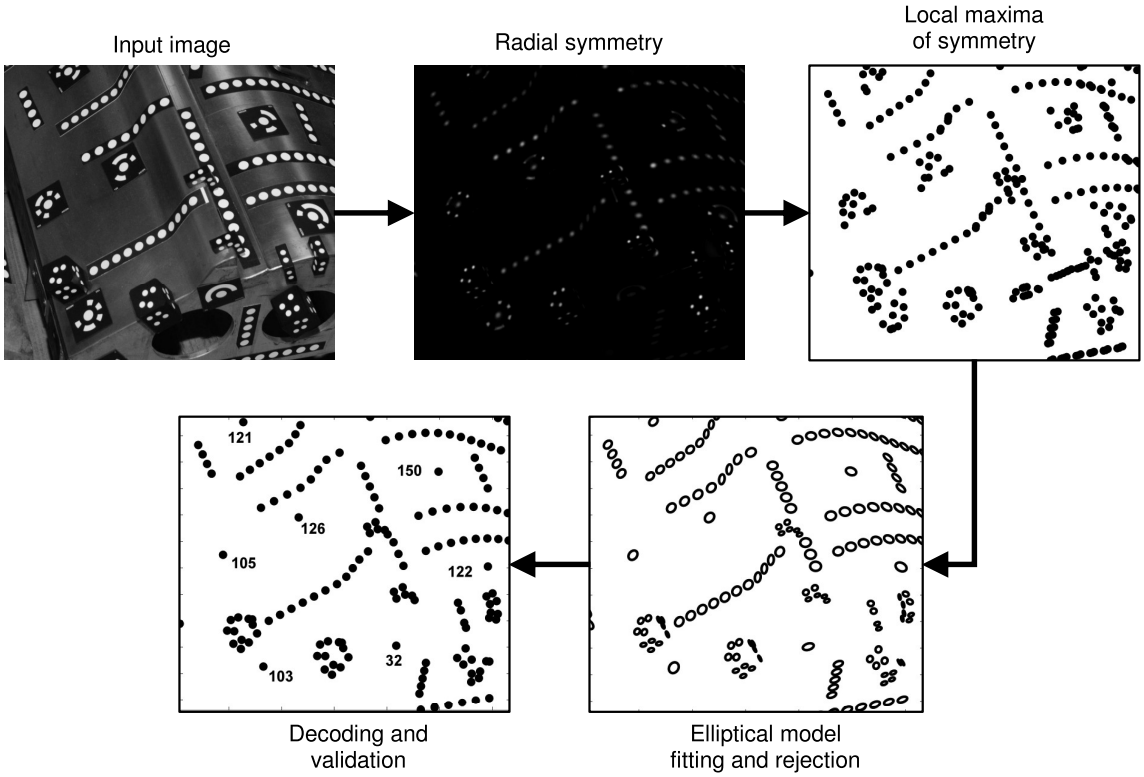

Figure 3. General diagram of the proposed method.

2. Target location

2.1 Elliptical blob detector

As said before, the selection of landmark candidates is performed by computing the local maxima of the response to a radial symmetry detector. The first step in the computation of radial symmetry consists in multiresolution decomposition of the image into a set of band-passed features. To this end we choose a bank of scaled and oriented log Gabor filters [9]. Log Gabor filters show many advantageous properties [10]. In particular, we have chosen them because, unlike Gabor filters, they have a zero DC component, and also because their response is better localized in the spatial domain. The log Gabor filter does not have an analytical expression in the spatial domain. In the spectral domain, its transfer function T is usually defined in polar frequency coordinates, and parameterized by the frequency and orientation coordinates, ρ_i and ϕ_j, of its peak, and the corresponding radial and angular widths, $\sigma_{\rho i}$, and $\sigma_{\phi j}$, as follows [9]

$$T_{ij}\left(\rho,\phi;\rho_i,\phi_i,\sigma_{\rho i},\sigma_{\phi i}\right)=\exp\left(-\frac{\log\left(\rho/\rho_i\right)^2}{2\log\left(\sigma_{\rho i}/\rho_i\right)^2}-\frac{\left(\phi-\phi_j\right)^2}{2\sigma_{\phi j}^2}\right) \quad (1)$$

The response R_{ij} of one of these filters to an input image I in the spatial domain is complex valued, with the real and imaginary components representing even and odd phase features respectively, with scale $\lambda_i=2/\rho_i$ and orientation ϕ_j. It can be rapidly computed in the frequency domain using the Discrete Fourier Transform DFT and its inverse IDFT, using the following expression, which is a straightforward derivation from the well known mathematical fact that states that a convolution in the spatial domain corresponds to a product in the Fourier domain.

$$R_{ij} = \mathrm{IDFT}\left(T_{ij} \cdot \mathrm{DFT}(I)\right) \tag{2}$$

Circular targets are even features, since we are interested in the whole region, and not only its border. Therefore, only the real component of the response $\Re\{R_{ij}\}$ will be used.

The bank of filters used here is designed to evenly cover the spectral domain. We choose to use a fixed number N_s of scales, with wavelengths in the range of interest $[\lambda_{\min},\lambda_{\max}]$. This interval is sampled with geometrically increasing values, so that $\lambda_i=\lambda_{\min}M^{i-1}$, with $M=(\lambda_{\max}/\lambda_{\min})^{1/(Ns-1)}$ being the ratio between consecutive scales. In our experiments N_s = 8, $\lambda_{\min}$=5 pixels and $\lambda_{\max}$ is 1/8 the size of the image, while $\sigma_{\rho i}$ is computed for each scale in order that the bandwidth is 2 octaves. The number of orientations has been set to N_o=4, with $\sigma_{\phi j}=\pi/N_o$.

From the band-passed features $\Re\{R_{ij}\}$, a scale space of radial symmetry is computed as the product of all oriented responses with same scale. Previous to product computation, prior knowledge about contrast of the targets is exploited in order to eliminate responses due to spots with opposite contrast. As a result, the response is inverted depending on contrast, and half wave rectified –negative values are set to zero. Hence, if c is the contrast of the targets (1 for white targets, −1 for black targets), then the symmetry measure S for scale i is

$$S_i = \prod_j \max(0, c\Re\{R_{ij}\}) \tag{3}$$

The overall radial symmetry is obtained from the radial symmetry scale-space by selecting the largest symmetry value over scales at each image point.

$$S(x,y) = S_{i=\hat{i}(x,y)}(x,y), \quad \text{where} \quad \hat{i}(x,y) = \arg\max_i \{S_i(x,y)\} \tag{4}$$

The method for the computation of multiresolution symmetry is depicted in Figure 4.

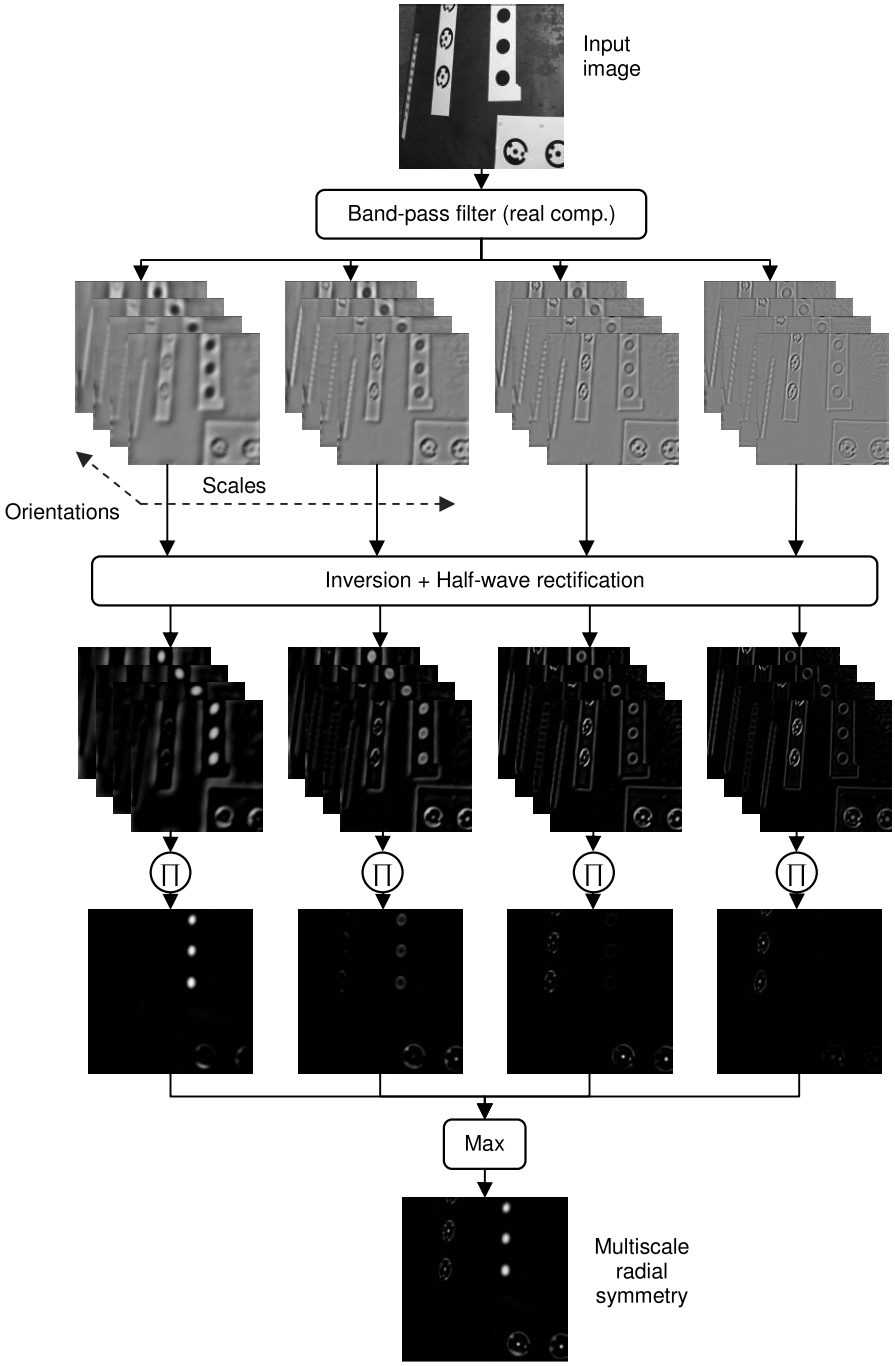

Figure 4. Sequence of processes for the detection of elliptical regions through the estimation of multiresolution radial symmetry –to simplify the figure, only four scales are used in this diagram, instead of 8.

2.2 Subpixel location

A first approach to the location of targets is provided by the local maxima of the multiresolution symmetry. An image point is classified as a maximum of symmetry if its value is larger than all other values in its 5x5 square neighborhood –the size of the

neighborhood has been selected empirically. Maxima are thresholded to retain only the strongest peaks. The threshold is computed automatically from the output of the detector previous to non-maxima suppression, as the mean plus the standard deviation of the multiresolution symmetry in the whole image.

To determine if a symmetry maximum actually corresponds to a circular target, and to precisely locate its center, it is necessary to analyze its surrounding region. This stage differs from the one published in [12], with clearly improved results. Here, a square region of interest (ROI) is defined with size proportional to its corresponding scale $\lambda_i(x,y)$. This ROI is used to compute an image intensity threshold that reliably segments the area covered by the target. Once the target is segmented, the subpixel location of its center is accomplished by elliptical model fitting. This approach has proven to provide a good tradeoff between precision and computational cost compared to more sophisticated models –we are not concerned here with the precision of the location of the targets; see Gutiérrez y Armstrong [13] for a recent review and a comparison between several precision location methods. In order to preserve the shape of contours from smoothing, these have been extracted using mathematical morphology operations. A pixel is marked as contour unless its 4-connected neighbors are all inside or outside the segmented area. The method of Halir and Flusser [14], based on a least squares criterion, is then applied for ellipse fitting. This method has proven to be numerically stable and also fast, since it is not iterative.

Once target regions are fit to an elliptical model, a final thresholding is applied to the error of the fit in order to discard false positives. The error of the fit is computed as the average distance from contour points to the model. The algorithm described in [3] has been used for distance estimation. The error threshold has been set to 0.1 pixels in the stage previous to coded target recognition, to avoid rejection of true targets. After recognition, targets identified as non-coded are thresholded again, now with a threshold of 0.05 pixels –precision of the detector is favored at the expense of sensitivity, since bundle adjustment techniques are highly sensitive to false positives.

3. Coded target recognition

Since the ratio between the radii of the target circumferences is known, once an elliptical model is available for the central spot of the target, it is straightforward to extract the region occupied by the coded ring. To simplify posterior computations, the

image is normalized as illustrated in Figure 5. The elliptical ring is mapped into a circular region of unit radius, by means of an inverse affine transformation, and then mapped to polar coordinates. Finally, intensity is normalized to the range [0,1].

The normalized rectangular image of the ring is decoded to get the corresponding binary sequence using standard segmentation techniques. The procedure adopted here involves taking the intensity maximum in the radial dimension –vertical coordinate in the normalized image– to get a one-dimensional profile. This operation provides a one-dimensional representation of the sequence that is robust to deviations from ellipticity, without the need of precisely determining the central radius of the ring [2].

The one-dimensional profile is then thresholded to get the binary sequence. The threshold level is computed as the average of the maximum and minimum intensity levels of the profile. Given the known number of bits of the codification and the selected contrast –black over white or vice versa– it is easy to determine the binary sequence of the ring. Finally, to get the numerical code of the target, the binary sequence and all its possible binary shifts are searched in a look-up-table (LUT). If the sequence is not found in the LUT, then the target is classified as non-coded. To avoid false positives, the obtained numerical code is tested by comparing the actual ring image with a synthetic phantom image. Here, similarity is estimated using the correlation coefficient. If the correlation is under a given threshold the target is classified as non-coded. The correlation threshold has been set to 0.75 in all experiments.

Finally, the estimation of the axis of the ellipse may not be exact due to large perspective distortions. This may lead to false negatives, as a consequence of the wrong estimation of the ring region. To cope with this problem, the whole segmentation process is performed for a range of values around the estimated axis of the ellipse. In this way, a search space is defined, constrained by the initial estimation. This procedure provides robustness to the classification method regardless of the correction in the elliptical fitting step.

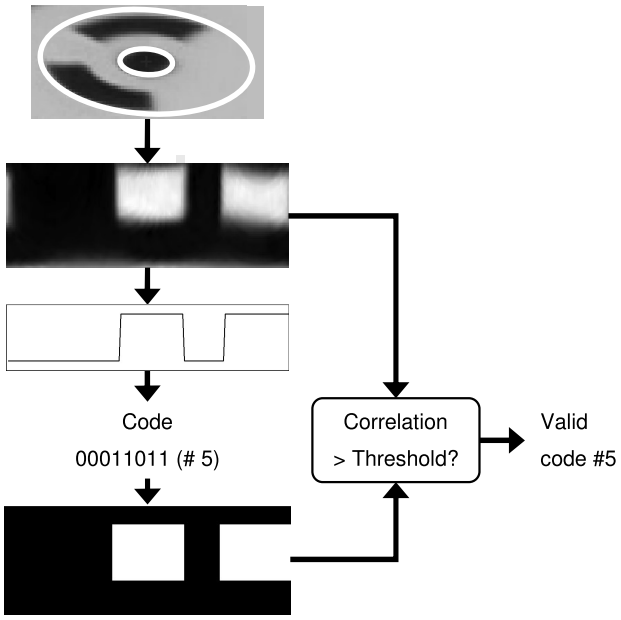

Figure 5. Target decoding process. From top to bottom: 1) Input image, a Photomodeler Scanner coded target of 8 bits, detected in the location step. The inner white circle represents the obtained elliptical model in the fitting stage. The outer white circle is computed from the inner one using the known ratio between them in the Photomodeler coding scheme. 2) Normalized coded ring region. 3) One-dimensional profile resulting from taking the maximum in the radial dimension and thresholding the normalized ring image. 4) Binary code associated to the previous profile, which corresponds to #5 in the LUT of the 8-bit Photomodeler codification scheme. 5) Synthetic coded ring computed for code #5 of the 8-bit Photomodeler codification. In the final stage, the correlation coefficient between the synthetic and real ring image is computed. The target is labeled as coded only if the correlation is over a given threshold.

4. Validation

The targets used in our experiments are AICON 3D ® targets, both non-coded and coded with 12 and 14 bits, with white color over black background, although the results can be extrapolated to inverse contrast. AICON 12-bit codification has 147 different targets, while AICON 14-bit codification has 516 targets.

Targets have been printed on magnetic paper for their fixation on metallic pieces. Images used for validation correspond to a metallic piece placed on a room with non-controlled ambient light. A camera flash has been applied during image capture. Two series of 10 images have been captured, one for 12-bit targets and the other one for 14-bit targets. The employed camera is a Nikon Dx3, with 35mm full-frame sensor and 6048×4032 pixel resolution, and with a 28mm lens. Exposure time was 1/60 sec. and the ISO level was set to 500. For radial symmetry computation, images have been resized to 2808×1872 using Lanczos-2 interpolation.

Validation was made by measuring the efficiency of detection and classification using the F_1 *score* statistical parameter [15], which represents the tradeoff between sensitivity and precision. Sensitivity is defined as the fraction of targets that are correctly detected, while precision is the fraction of detected targets that correspond to actual targets. Therefore,

$$sensitivity = \mathrm{TP/P} = 1 - \mathrm{FN/P} \tag{5}$$

$$precision = \mathrm{TP/(TP+FP)} \tag{6}$$

$$F_1^{-1} = (sensitivity^{-1} + precision^{-1})/2 \tag{7}$$

where P is the total number of targets, FP is the number of false positives of detection –points that are incorrectly labeled as targets–, FN is the number of false negatives –true targets that have not been detected– and TP is the number of true positives –actual targets that are correctly detected. F_1 *score* values range from zero, when either sensitivity or precision are zero, to one, when both of them are maximal. For validation of the classification results, incorrectly labeled targets are considered both FP and FN, since they indicate an error in both the actual classifier and the winner classifier.

Sensitivity and precision values vary as a function of the chosen fitting error threshold, such that a large threshold ensures high precision at the expense of sensitivity and vice versa. The F_1-*score* represents the tradeoff between both parameters, so that it provides results that are less dependent on the chosen threshold. Still, F_1-*score* is not completely independent on the threshold, as seen in Figure 6. All results shown in this paper have been obtained using a fitting error threshold of 0.05 pixels, except from the results provided by the AICON system.

Tables 1 and 2 show efficiency results for the proposed method of target detection for both coded and non-coded targets. The same results are graphically represented in Figure 7. The obtained results have been compared to the ones provided by the AICON system. In the same way, Table 3 and 4 show the classification results obtained for 12-bit and 14-bit codifications, which are represented in Figure 8. Figure 9 shows detection and classification results for three example images for both the proposed method and the AICON system.

Detection results prove that the method proposed here, based on a new estimation of radial symmetry, behaves well under ambient illumination conditions. Besides, the targets in the test images present perspective distortions, noise, different sizes and even slight defocusing. Despite all of this, sensitivity results outperform the ones from the

AICON system, while precision values are preserved. This yields an overall improved performance. The same applies for the decoding method used for classification of coded targets.

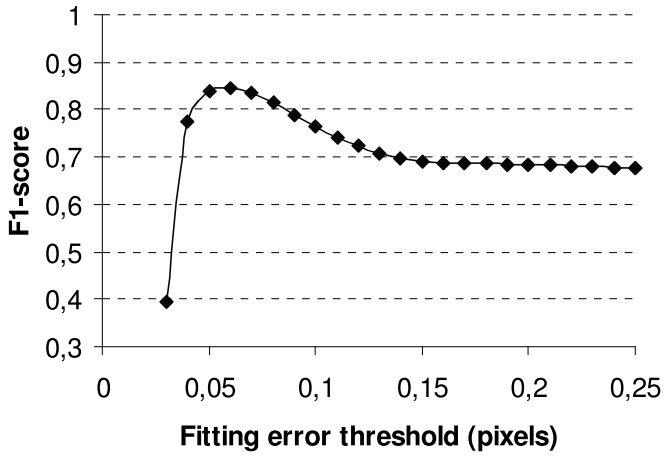

Figure 6. F_1-*score* of detection for images of series #1 as a function of the elliptical fitting error threshold.

Table 1. Efficiency results obtained in the detection stage for targets of the series #1, corresponding to 10 images with AICON targets. Results are provided for the proposed method, based on radial symmetry, and for the AICON system.

Series #1	Sensitivity	Precision	F_1-*score*
Radial Symmetry	0.857	0.985	**0.916**
AICON	0.367	0.997	0.537

Table 2. Efficiency obtained in the detection stage for targets of the series #2, also with 10 images.

Series #2	Sensitivity	Precision	F_1-*score*
Radial Symmetry	0.733	0.991	**0.843**
AICON	0.634	0.978	0.769

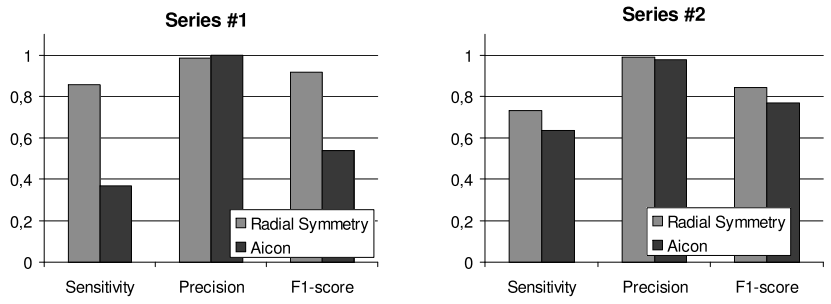

Figure 7. Representation of the efficiency data from Tables 1 and 2.

Table 3. Efficiency of coded target classification for images in series #1, corresponding to 10 images showing 12-bit coded AICON targets.

12 bits	Sensitivity	Precision	F_1-*score*
Decodification	0.672	0.968	**0.794**
AICON	0.656	0.994	0.790

Table 4. Efficiency of coded target classification for images in series #2, corresponding to 10 images showing 14-bit coded AICON targets.

14 bits	Sensitivity	Precision	F_1-*score*
Decodification	0.748	0.991	**0.852**
AICON	0.544	0.997	0.705

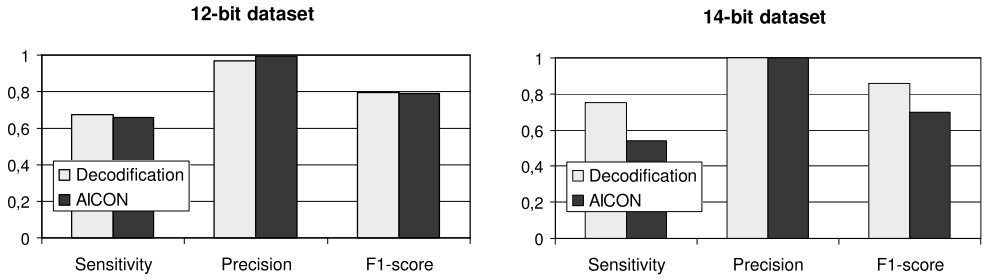

Figure 8. Classification results from Tables 3 and 4, obtained with the proposed method and with the AICON system, for both 12-bit and 14-bit image sequences.

5. Conclusions

This paper has presented an efficient methodology for the detection of circular photogrammetric targets, their precise location and their identification. Target candidate selection is based on a novel measure for radial symmetry. The proposed radial symmetry operator combines information from the responses of a bank of scaled and oriented filters to build a scale-space of product of orientations. Such scale-space provides a multiresolution blob detector with a narrow point-spread function, which is robust to perspective distortion and target size. Precision location is accomplished by means of elliptical model fitting. Finally, coded target recognition is performed by decoding the binary sequence in the outer ring of the target, using simple segmentation techniques that exploit the geometry of the codification.

The method is robust under ambient illumination conditions and presence of background clutter. Compared to a commercial photogrammetry system, the AICON 3D, the presented methodology provides higher detection and classification sensitivities, while preserving precision. As a result, its overall efficiency, measured as the balance between these two statistics by means of the F_1-score, outperforms the commercial system.

Acknowledgments

This work has been developed in the framework of the projects Alexandria (Ref. PSE-020000-2009-10) and DICON (Ref: IPT-2011-1191-020000), funded by the Spanish *Ministerio de Ciencia e Innovación*, under the programs *Proyectos Singulares Estratégicos* and *INNPACTO* respectively. We also acknowledge the *Laboratorio Oficial de Metroloxía de Galicia* for providing test images and ground truth data.

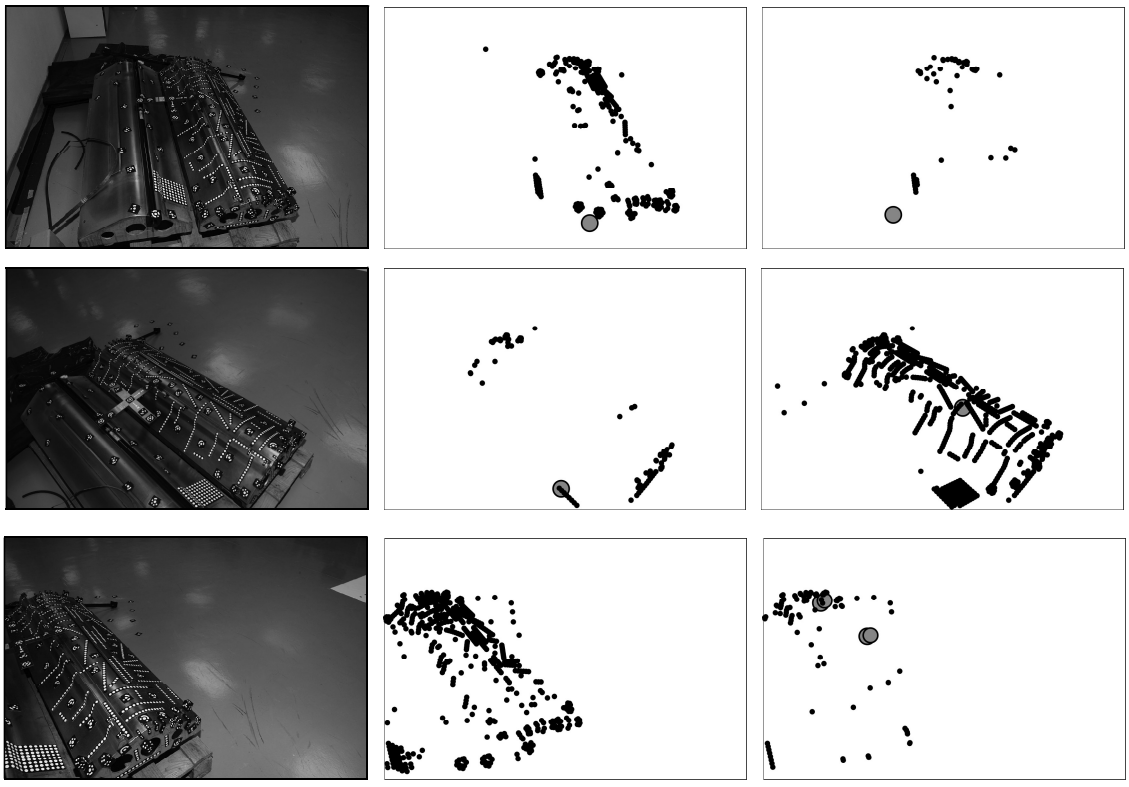

Figure 9. From top to Bottom: three examples of detection with images from series #2. *Left*: Input images. *Middle*: AICON errors. *Right*: errors of the proposed method. Black dots indicate false negatives (FN) of detection and gray circles indicate false positives (FP) of detection. The AICON system shows many false negatives, but few false positives. Our method shows low number of both false positives and false negatives. As a consequence, the F_1-*score* values are generally larger.

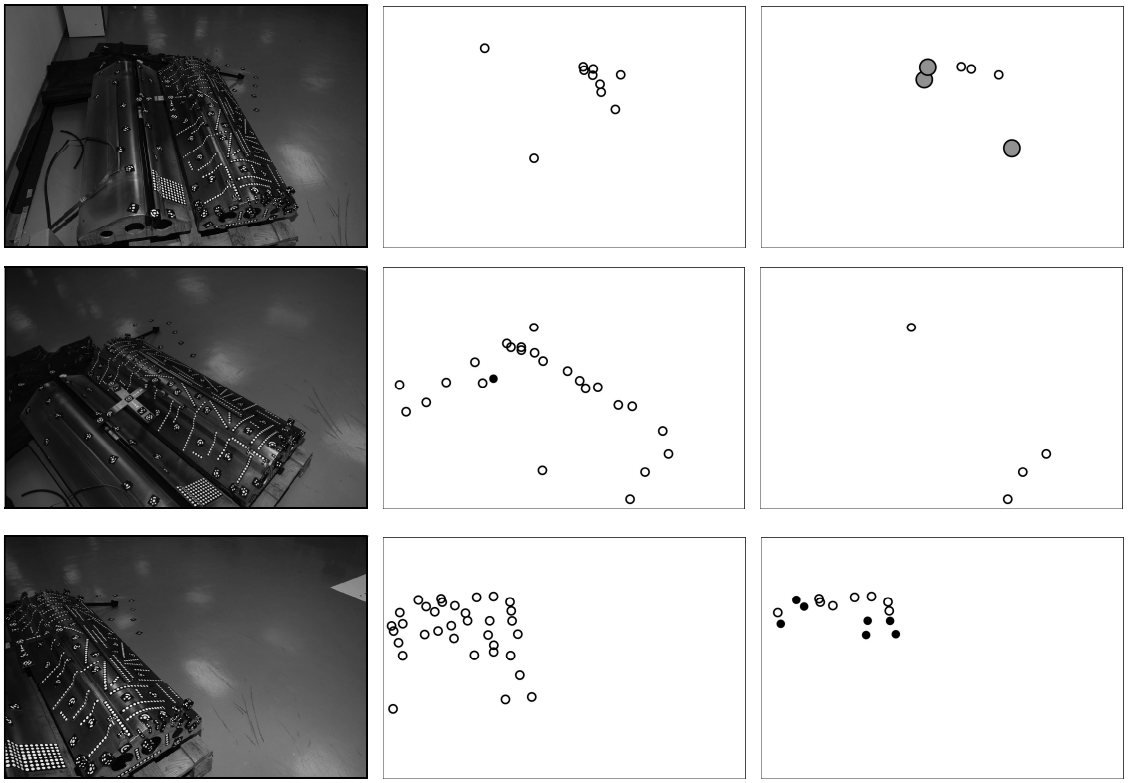

Figure 10. From top to Bottom: three examples of classification with images from series #2. *Left*: Input images. *Middle*: AICON errors. *Right*: errors of the proposed method. Black dots are classification false negatives (FN) and gray circles are classification false positives (FP, non coded targets which are assigned a code). In these examples there are no wrong classification errors (coded targets which are assigned a wrong code). There are some coded targets that have not been subject to classification due to a previous error in the detection stage. They are marked with small white circles, and they are not considered as FP in the evaluation of the F_1-*score* of classification. In general there are few classification false positives although, occasionally, our method wrongly assigns a code to non coded targets, like in the first example. However, the sensitivity is clearly higher in the proposed method, resulting in a higher F_1-*score.*

References

[1]. Ahn SJ, Rauh W, Recknagel M (1999) Circular coded landmark for optical 3D-measurement and robot vision. Conf. on Intelligent Robots and Systems (IROS'99), pp. 1128-1133. DOI 10.1109/IROS.1999.812831

[2]. Chen Z, Ye Z, Chan DTW, Peng G (2007) Target Recognition Based on Mathematical Morphology. CAD/Graphics'07, pp. 457-460. DOI 10.1109/CADCG.2007.4407929

[3]. Otepka JO, Hanley HB, Fraser CS (2002) Algorithm Developments For Automated Off-Line Vision Metrology. Int. Archives of Photogrammetry & Remote Sensing, 5:60-67

[4]. Shortis MR, Clarke TA, 1994. Comparison of some techniques for the subpixel location of discrete target images. Proc. SPIE, Viometrics III, 2350:239-250

[5]. Knyaz VA, Sibiryakov AV (1998) The Development of New Coded Targets for Automated point Identification and Non-contact 3D Surface Measurements, Int. Archives of Photogrammetry and Remote Sensing, 32(5):80-85

[6]. Lowe, D.G. Distinctive image features from scale-invariant keypoints. Int. Journal of Computer Vision, 60(2):91-110, 2004.

[7]. Loy G, Zelinsky A (2003) Fast Radial Symmetry for Detecting Points of Interest, PAMI 25:959-973

[8]. Nixon MS, Aguado AS (2008) Feature Extraction and Image Processing. Academic Press, Oxford

[9]. Field DJ (1993) Scale–Invariance and self-similar "wavelet" Transforms: An Analysis of Natural Scenes and Mammalian Visual Systems. In Farge M et al (eds). Wavelets, fractals and Fourier Transforms, Clarendon Press, Oxford, pp. 151-193

[10]. Kovesi, P. Invariant Measures of Image Features from Phase Information. Ph.D. Thesis, University of Western Australia, 1996.

[11]. Eberly D (2004) Distance from a point to an ellipse in 2D. Geometric Tools, LLC, www.geometrictools.com.

[12]. Dosil R, Pardo XM, Fdez-Vidal XR, Garcia-Diaz A, Leborán V (2010) A New Multiresolution Blob Detector Applied to Photogrammetry. In Pérez JC (ed.). III Congreso Español de Informática, Ibergarceta, Madrid, pp. 109–116

[13]. Gutierrez JA, Armstrong BSR (2008) Precision Landmark Location for Machine Vision and Photogrammetry. Springer, London

[14]. Halir R, Flusser J (2000) Numerically Stable Direct Least Squares Fitting of Ellipses. Department of Software Engineering, Charles University, Czech Republic

[15]. van Rijsbergen, C. J. (1979). Information Retrieval. Butterworth.